ISSN 1070-4272, Russian Journal of Applied Chemistry, 2017, Vol. 90, No. 10, pp. 1712−1721. © Pleiades Publishing, Ltd., 2017.
Original Russian Text © R.R. Mansurov, A.P. Safronov, N.V. Lakiza, I.V. Beketov, 2017, published in Zhurnal Prikladnoi Khimii, 2017, Vol. 90, No. 10, pp. 1399−1409.

MACROMOLECULAR COMPOUNDS AND POLYMERIC MATERIALS

Photocatalytic Activity of Titanium Dioxide Nanoparticles Immobilized in the Polymer Network of Polyacrylamide Hydrogel

R. R. Mansurov[a]*, A. P. Safronov[a,b], N. V. Lakiza[a], and I. V. Beketov[a,b]

[a] *Ural Federal University, pr. Lenina 51, Yekaterinburg, 620075 Russia*
[b] *Institute of Electrophysics, Ural Branch, Russian Academy of Sciences, ul. Amundsena 106, Yekaterinburg, 620016 Russia*
e-mail: renat.mans@gmail.com

Received October 31, 2017

Abstract—Composite hydrogels based on polyacrylamide immobilized nanoparticles of commercial (P25 brand) titanium dioxide and of titanium dioxide nanoparticles prepared by electric explosion of a wire were synthesized. The enthalpy of interaction at the polyacrylamide/TiO_2 interface was determined by microcalorimetry using the thermochemical cycle method. Interaction of polyacrylamide polymer chains with the surface of TiO_2 nanoparticles is energetically unfavorable. The absence of interactions between the hydrogel polymer network and surface of TiO_2 nanoparticles favors manifestation of the UV-induced photocatalytic activity of TiO_2 nanoparticles immobilized in the hydrogel. Immobilization in the polyacrylamide hydrogel matrix decreases the photocatalytic activity of P25 brand TiO_2 nanoparticles, but does not affect the photocatalytic activity of titanium dioxide nanoparticles prepared by the electric explosion method. The photocatalytic activity of TiO_2 nanoparticles immobilized in the bulk of polyacrylamide hydrogel evaluated by the decomposition of Methyl Orange dye is controlled by the diffusion rate of the dye molecules into the bulk of the hydrogel and depends also on the aggregation of TiO_2 nanoparticles in the hydrogel matrix.

DOI: 10.1134/S1070427217100238

The photocatalytic activity of titanium dioxide nanoparticles was discovered in the 1960s, and interest in it not only does not weaken but even tends to increase [1]. Hydrogen generation by photocatalytic water splitting, photocatalytic reduction of carbon dioxide to hydrocarbons, photocatalytic organic synthesis reactions, photocatalytic air and water treatment to remove organic pollutants and pathogenic bacteria—all these process are possible when the photocatalyst is irradiated merely with sunlight [2]. Nanodispersed titanium dioxide is an optimum photocatalyst owing to its cheapness, physicochemical stability, and high performance [1]. A number of procedures for improving the functional properties of nanodispersed titanium dioxide were suggested in the course of more than half-century studies of this material. In particular, the problem of low photocatalytic activity (PA) under sunlight can be successfully solved today by the creation of the heterostructure in titanium dioxide nanoparticles [3, 4].

However, despite increased researchers' interest, photocatalysis has not yet found wide use in practice. There are a number of problems specific for each application. For example, photocatalytic treatment of water using TiO_2 nanoparticles is formed a stable aqueous suspension whose coagulation requires much energy [5]. To solve this problem, attempts are made to immobilize nanoparticles in various matrices, including polymer matrices [5, 6]. The following advantages of polymer matrices are noted: They exhibit physicochemical stability, are readily available, and can be readily processed into various forms. Furthermore, polymer matrices can be readily sensitized with various organic dyes to enhance the light absorption in the visible range of the solar spectrum [7].

As noted by Lei et al. [8], hydrophilic polymers, in particular, polyvinyl alcohol, are the best matrices for immobilizing TiO_2 nanoparticles for photocatalytic water treatment to remove organic pollutants. Lei et al. believe that this is caused by an increase in the contact surface area of TiO_2 nanoparticles and dye molecules due to partial swelling of the polymer in an aqueous medium. Therefore, it seems promising to use as an immobilizing matrix polymer hydrogels exhibiting increased swelling in aqueous medium. Polymer hydrogels are cross-linked polymers based on hydrophilic macromolecules capable of equilibrium and reversible swelling in aqueous media. Hydrogels exhibit a number of unique properties making them "smart materials"; for example, the degree of their swelling depends on temperature, pH, and ionic strength of the medium [9]. Thus, the possible functions of the hydrogel matrix are not restricted to immobilization or sensitization of TiO_2 particles; it can also enrich the physicochemical properties of the photocatalyst as a component of the composite material.

The photocatalytic activity of titanium dioxide nanoparticles immobilized in the polymer network of hydrogels based on various polymers has been studied. These polymers include polyacrylamide and its copolymers [10–14], poly-N,N-dimethylacrylamide [15], polyvinyl alcohol and its copolymers [16, 17], and chitosan and its copolymers [18]. Polymerization is usually performed in the bulk, but Morsi and Elsalamony [14] prepared core–shell nanocomposite particles by inversion emulsion polymerization in situ. In [16, 17], composite hydrogels were prepared in the form of fibers by electrospinning method. Nevertheless, irrespective of the matrix and synthesis method used, TiO_2 nanoparticles immobilized in the polymer network of a hydrogel were found to exhibit photocatalytic activity manifested in decolorization of various organic dyes in aqueous medium under UV irradiation.

However, the available papers usually report the very fact of the photocatalytic activity (PA) of composite hydrogels without attempting to account for this phenomenon. The photocatalytic activity of TiO_2 nanoparticles is commonly known, but its preservation upon incorporation of nanoparticles into a polymer matrix is not obvious. Photocatalysis is a kind of heterogeneous catalysis; therefore, the photocatalytic activity is possible only on the surface of photocatalyst nanoparticles [1]. When a photocatalyst is incorporated in a polymer matrix, its active surface will interact to a certain extent with the polymer matrix of the hydrogel, which should inevitably affect the PA of TiO_2 nanoparticles and can lead even to its disappearance due to adsorption of macromolecules on the nanoparticle surface.

We have found only two papers in which the authors attempt to account for the PA of titanium dioxide nanoparticles immobilized in the bulk of a hydrogel. Kazemi et al. [12] studied a composite hydrogel based on polyacrylamide and stated that the surface of TiO_2 nanoparticles in the bulk of the hydrogel was completely shielded by macromolecules of the polymer network, so that only TiO_2 nanoparticles located on the hydrogel surface exhibited PA. On the other hand, Im et al. [16] studied a composite hydrogel based on polyvinyl alcohol and suggested a mechanism of the photocatalytic decomposition of organic dye molecules on the surface of immobilized TiO_2 nanoparticles, based on diffusion of dye molecules to the nanoparticle surface via hydrogel volume. Thus, the question as to whether TiO_2 nanoparticles immobilized in the hydrogel volume can exhibit photocatalytic activity still remains open. The answer to this principal question largely depends on the nature of interaction of the hydrogel polymer network with the surface of photocatalyst nanoparticles. Evaluation of this interaction is necessary for comprehensive understanding of the photoinduced physicochemical processes occurring in the composite hydrogel at the interface between the photocatalyst nanoparticle surface and the hydrogel polymer network. Such evaluation has not been done in the previously published papers.

This study deals with the effect exerted by interfacial interaction of the polymer network of polyacrylamide hydrogel with the surface of titanium dioxide nanoparticles on the photocatalytic activity of the composite hydrogel. We have studied the chemically cross-linked polyacrylamide hydrogels filled with different kinds of titanium dioxide nanoparticles: those of commercial (P25 brand) titanium dioxide and those prepared by electric explosion of a wire. The photocatalytic activity of both samples of TiO_2 nanoparticles was characterized by us previously.

EXPERIMENTAL

Characteristics of TiO_2 nanopowders. We used as photocatalysts P25 brand titanium dioxide nanoparticles

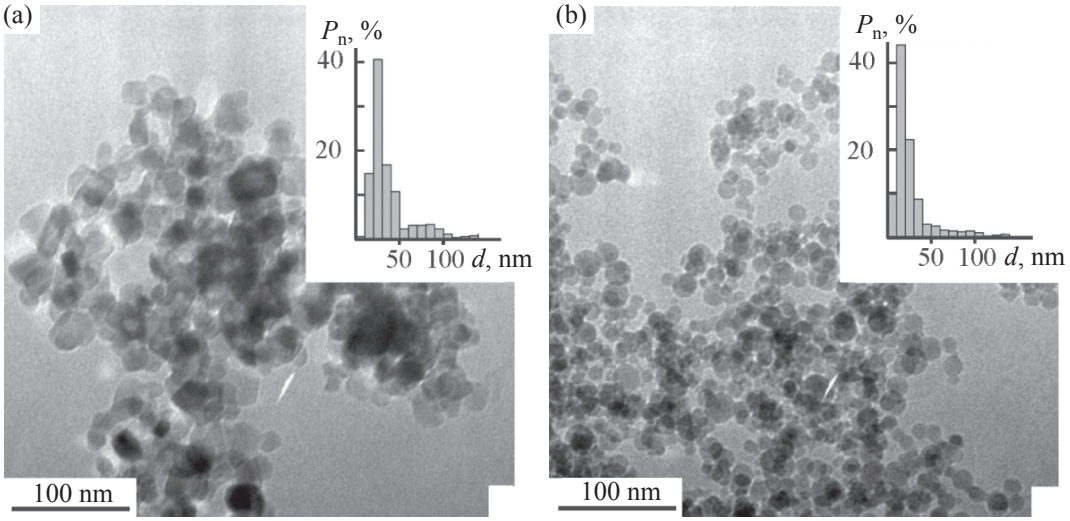

Fig. 1. Electron micrographs of (a) TiO_2-P25 and (b) TiO_2-EEW nanopowders. The inserts show the nanoparticle size distribution: (d) nanoparticle size and (P_n) numerical fraction.

produced by Evonik (TiO_2-P25) and nanoparticles prepared by electric explosion of the wire (TiO_2-EEW) at the Institute of Electrophysics, Ural Branch, Russian Academy of Sciences. The characteristics of the TiO_2 nanopowders are given in Table 1. The specific surface area S_{sp} of the nanopowders was determined by the BET method from low-temperature equilibrium adsorption of nitrogen vapor on a Micromeritics TriStar 3020 vacuum sorption installation. The mean particle size, d_{BET}, was calculated from the BET data using the formula for spherical particles [19]:

$$d_{BET} = \frac{6}{\rho S_{sp}},$$

where ρ is the theoretical crystallographic density of the nanopowder.

The electron micrographs of the nanopowders were taken with a JEOL JEM 2100 transmission electron microscope (TEM). The electron micrographs of TiO_2 nanopowders are shown in Fig. 1. For both nanopowders, the particle size distribution was determined by graphic analysis of the electron micrographs, assuming the spherical particle shape, and the mean particle size was calculated from these data (Table 1).

As seen from Fig. 1, TiO_2-EEW nanoparticles have spherical shape, and TiO_2-P25 nanoparticles, approximately spherical shape. The TiO_2-EEW nanoparticles have a smaller size and are weakly agglomerated, whereas TiO_2-P25 nanoparticles are partially agglomerated.

The phase composition of the powders was characterized by X-ray diffraction analysis (XRD) with a Bruker D8 Discover diffractometer in copper radiation with a graphite monochromator on the diffracted beam. The data were processed using the TOPAS 2.1 program with Rietveld refinement of the parameters. The phase composition of the samples is given in Table 1. For both samples, the anatase phase prevails. According to

Table 1. Characteristics of titanium dioxide nanoparticles[a]

Sample	ρ, g cm^{-3}	S_{sp}, m^2 g^{-1}	d_{BET}	d^n (TEM)	d^w (TEM)	Content of indicated phase, %	
			nm			rutile	anatase
TiO_2-P25	4.07	45.2	33	39	115	12	88
TiO_2-EEW	4.10	47.3	31	29	118	28	72

[a] d^n(TEM) is the number-average, and d^w(TEM), weight-average nanoparticle size determined by graphic analysis of electron micrographs.

published data [1], it is favorable for the manifestation of the photocatalytic activity of TiO_2 nanoparticles. As seen from Table 1, the anatase phase content is higher for the TiO_2-P25 sample.

Synthesis of composite hydrogels. Hydrogels were synthesized at room temperature by radical polymerization of acrylamide (Merck) in 1.6 M aqueous solution. To create the three-dimensional network structure of the hydrogel, we used N,N-methylenediacrylamide (Merck) as a cross-linking agent. Its concentration in aqueous solution was 0.016 M. The ratio of the monomer and cross-linking agent (degree of cross-linking), set by the synthesis conditions, was 1 : 100. A 10 g L^{-1} aqueous suspension of TiO_2 nanoparticles was prepared separately with a Cole Palmer CPX 750 ultrasonic disperser. Ultrasonic treatment was performed for 15 min at an output power of 150 W. The particle size distribution in aqueous suspensions was monitored by dynamic light scattering with a Brookhaven Zeta Plus universal particle size analyzer. The suspension was introduced into the reaction mixture in an amount ensuring 0.25 wt % content of TiO_2 nanoparticles in the ready composite hydrogel. Ammonium persulfate (5 mM) was used as a polymerization initiator, and *N,N,N'*,*N'*-tetramethylmethylenediamine (Merck) served as a polymerization accelerator. Synthesis was performed in glass capillaries 2 mm in diameter at room temperature. The synthesized composite hydrogel was washed for 2 weeks with distilled water to remove oligomeric fractions and reach the equilibrium swelling. The degree of swelling α was calculated by the formula

$$\alpha = \frac{m_s - m_d}{m_d},$$

where m_s is the weight of the swollen hydrogel and m_d is the weight of the hydrogel dried to remove water.

Determination of the photocatalytic activity of TiO_2 nanoparticles immobilized in the hydrogel. The photocatalytic activity of TiO_2 nanoparticles immobilized in the hydrogel was evaluated by decolorization of Methyl Orange (MO) dye in aqueous solution under the action of artificial radiation at a fixed distance of 35 mm. MO was of chemically pure grade. A gel sample in the form of a 45 × 2.9 mm cylinder (V = 0.32 mL) was placed in a polypropylene cell containing 12 mL of a 3 μM aqueous MO solution and was left for 24 h in the dark to reach the equilibrium. The pH of the aqueous medium immediately before the irradiation was 6.5. Irradiation was performed with stirring using a magnetic stirrer. The hydrogel sample freely moved in the cell volume. A 3-W light-emitting diode was used as a UV radiation source. Its radiation spectrum had a peak near 365 nm. The luminous flux intensity was 5 mW cm^{-2}. After the irradiation, the cell was sealed and left for 24 h in the dark to reach the equilibrium. The residual MO concentration in the aqueous solution was determined spectrophotometrically with a Helios Alpha spectrophotometer (Thermo Fisher Scientific) at a wavelength of 464 nm, corresponding to the MO absorption maximum, using the preliminarily constructed calibration plot.

To evaluate the effect of the immobilizing hydrogel matrix on PA of TiO_2 nanoparticles, we measured PA of individual TiO_2 nanoparticles. To this end, we prepared a suspension of TiO_2 nanoparticles in 12 mL of a 3 μM aqueous MO solution, stirred with a magnetic stirrer for 15 min, and left in the dark for 1 h to reach the adsorption equilibrium. The total gravimetric content of nanoparticles in the suspension was the same as the total content of nanoparticles in the ready sample of the composite hydrogel taken for PA determination. The suspensions were irradiated under the same conditions as the composite hydrogel samples. After the irradiation, the suspensions of TiO_2 nanoparticles were separated by centrifugation for 15 min at 9000 rpm. The residual MO concentration in the aqueous solution after the UV irradiation was determined by the similar spectrophotometric procedure.

The data on the photocatalytic activity of TiO_2 nanoparticles were processed using the pseudo-first-order equation [10]

$$-\ln (c/c_0) = k\tau,$$

where c_0 and c are the initial (taking into account adsorption) and residual MO concentrations in the aqueous solution, respectively; τ, irradiation time; k, effective constant of photocatalytic decomposition of Methyl Orange molecules.

Interfacial interaction between the TiO_2 nanoparticle surface and polyacrylamide. The enthalpy of adhesion of polyacrylamide polymer chains to the TiO_2 nanoparticle surface was studied using the thermochemical cycle. Model polyacrylamide/TiO_2 composites with the degree of filling from 0 to 100% (10% step) were prepared separately as follows. A weighed portion of the nanopowder was placed in a 10% aqueous solution

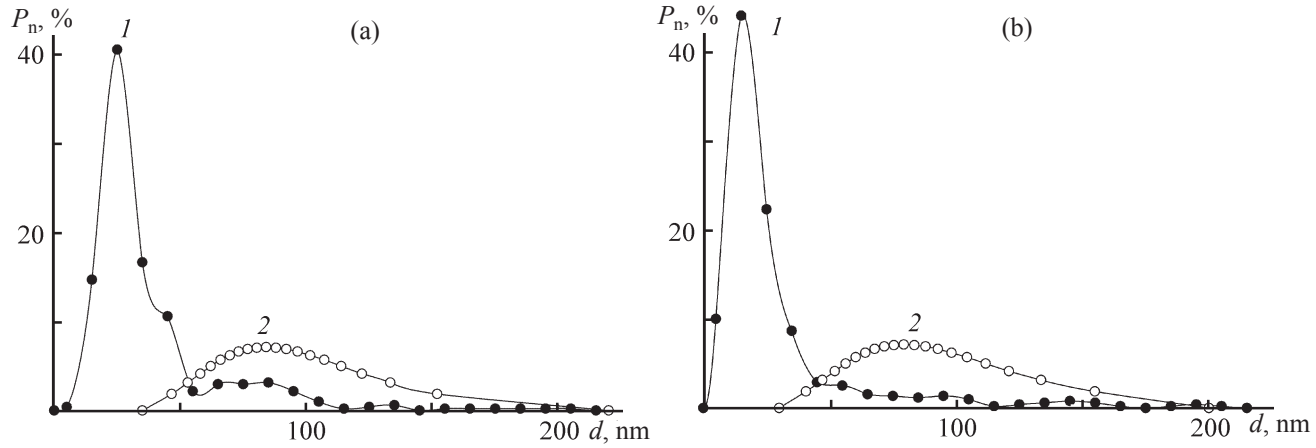

Fig. 2. Nanoparticle size distribution in the (*1*) initial nanopowders and (*2*) their aqueous suspensions for (a) TiO_2-P25 and (b) TiO_2-EEW nanoparticles. (*d*) Nanoparticle size and (P_n) numerical fraction.

of linear polyacrylamide and mechanically mixed in an agate mortar. The homogeneous mixture obtained was dried on a Teflon support to constant weight. A weighed portion of the composite prepared was placed in a 0.35-mL thin-walled glass ampule and dried in a vacuum to constant weight, after which the ampule was sealed. Then, the ampule was placed in a calorimetric chamber with 5 mL of water, which, in turn, was arranged in the calorimeter cell. The thermal effects of dissolution of the polymer and filled composites in water and the heats of wetting of TiO_2 nanopowders with water were measured on a microcalorimeter with an isothermal cell kept at 298 ± 0.1 K. The absolute uncertainty of the calorimetric measurement results, according to the electrical calibration data, was ±0.02 J.

RESULTS AND DISCUSSION

As described above, the hydrogels were filled using aqueous suspensions of TiO_2 nanoparticles. It is known that nanoparticles in aqueous medium tend to aggregation [20]. Therefore, the particle size distribution in a suspension can differ significantly from the distribution obtained by graphic analysis of electron micrographs of the initial nanopowders (Fig. 1). The particle size distribution in TiO_2 suspensions used for preparing nanocomposite hydrogels was characterized by dynamic light scattering method. Figure 2 shows the particle size distribution for the initial nanopowders, determined by graphic analysis of the electron micrographs, and for aqueous TiO_2 suspensions used for filling the hydrogels.

As seen from Fig. 2, for both nanopowder samples the number-average particle size in the suspension is larger than in the initial powder. Comparison of the particle size in suspensions with the TEM data shows that both TiO_2 powders tend to aggregation in aqueous medium to form nanoparticle aggregates with the diameter of approximately 80 nm.

The density of the network structure of composite hydrogels was evaluated by their equilibrium swelling degree in water using the Flory–Renner equation [21]. The equilibrium degree of swelling α of composite hydrogels coincided within the measurement uncertainty with the equilibrium degree of swelling of unfilled PAA hydrogel, 12 ± 0.5. From this value, we calculated the mean number of monomeric units between the cross-linking points, N_C [22]:

$$N_C = \frac{V_1(0.5\alpha^{-1} - \alpha^{-1/3})}{V_2[\ln(1-\alpha^{-1}) + \alpha^{-1} + \chi\alpha^{-2}]},$$

where V_1 and V_2 are the partial molar volumes of the solvent and polymer, respectively, and χ is the Flory–Huggins thermodynamic parameter of interaction of the polymer with the solvent.

The following values were used in the calculations: V_1 = 18 cm^3 mol^{-1} (for water), V_2 = 56.2 cm^3 mol^{-1} (for polyacrylamide), and χ = 0.12. The values of V_2 and χ were obtained by molecular modeling using CAChe 7.5 program package for quantum chemical modeling. The N_C value obtained was 53. This value corresponds to the mean number of monomeric units between the cross-linking points in the hydrogel. However, the mean distance between the cross-linking points cannot be calculated as a simple product of the number of

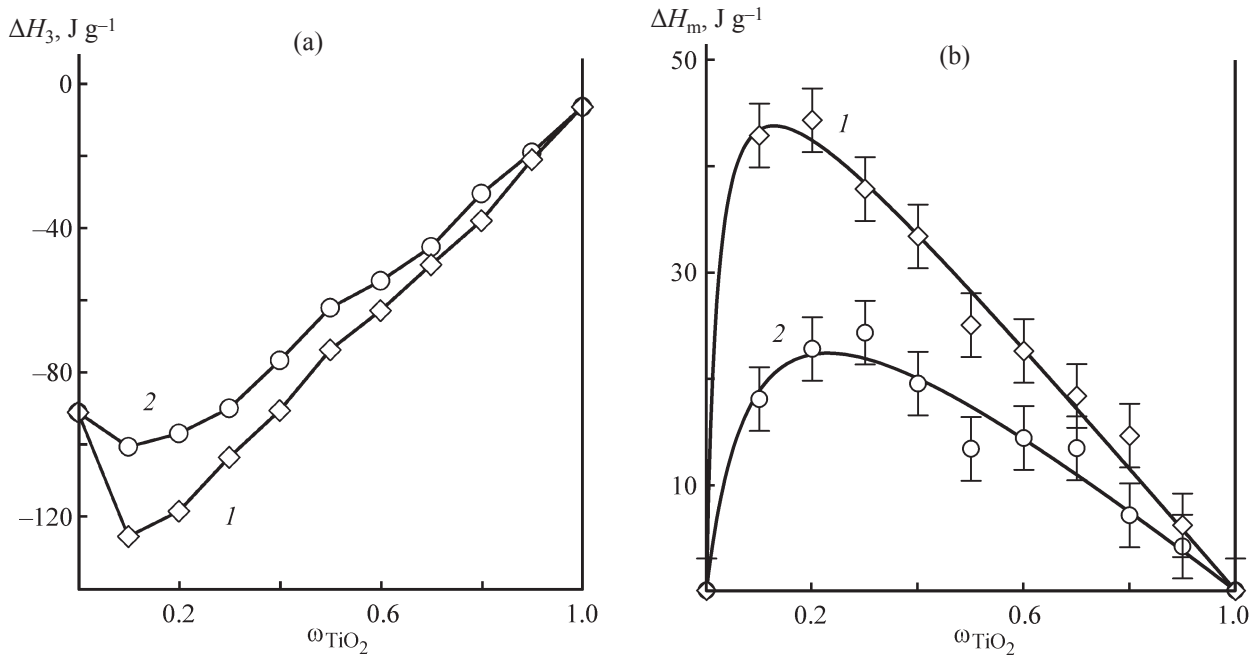

Fig. 3. (a) Enthalpy of dissolution ΔH_3 and (b) enthalpy of mixing ΔH_m as functions of the weight fraction ω_{TiO_2} of (*1*) TiO_2-P25 and (*2*) TiO_2-EEW nanoparticles in the polyacrylamide/TiO_2 composite.

monomeric units and the length of one unit because of the flexibility of the subchains between the cross-linking points. It is known that uncharged polymer (e.g., polyacrylamide) chains in an aqueous medium occur in the random coil conformation with braked rotation. The mean square of the distance between the termini of such a chain containing N units, each of length a, can be calculated using the equation [23]

$$\left\langle R^2 \right\rangle = \mathrm{Na}^2 \frac{1-\cos\vartheta}{1+\cos\vartheta},$$

where N is the number of bonds in a polymer chain, a is the chemical bond length, and ϑ is the chemical bond angle.

The following parameters of the C–C bond were used: a = 0.154 nm and ϑ = 109.5°. The number of bonds in the polymer chain, N, was equal to N_C. The calculated average distance between the cross-linking points was 4.0 nm, which is smaller by an order of magnitude than the mean diameter of TiO_2 nanoparticles according to TEM data (Table 1). It can be concluded that TiO_2 nanoparticles are completely immobilized in the network of the polyacrylamide gel and are incapable of translation mobility.

The interfacial interaction between the TiO_2 nanoparticle surface and polyacrylamide (PAA) subchains was studied by microcalorimetry method. The interaction of the nanoparticle surface with the PAA network in the composite can be described by the equation PAA + TiO_2 = PAA/TiO_2 composite + ΔH_m. The enthalpy of mixing, ΔH_m, could not be measured directly; therefore, we used the thermochemical cycle consisting of the following reactions:

(1) PAA + H_2O (excess) = dilute aqueous PAA solution + ΔH_1,

(2) TiO_2 + H_2O (excess) = aqueous TiO_2 suspension + ΔH_2,

(3) PAA/TiO_2 + H_2O (excess) = aqueous PAA solution with TiO_2 nanoparticles + ΔH_3,

(4) aqueous PAA solution + aqueous TiO_2 nanosuspension = aqueous PAA solution with TiO_2 nanoparticles + ΔH_4.

The Hess law equation for this set of reactions is as follows:

$$\Delta H_m = \omega_{PAA}\Delta H_1 + \omega_{TiO_2}\Delta H_2 + \Delta H_3 - \Delta H_4,$$

where ω_{PAA} and ω_{TiO_2} are the weight fractions of polyacrylamide and TiO_2 nanoparticles in the composite, respectively.

Because hydrogels are insoluble in water, the measurements were performed for model composites of TiO_2 with linear polyacrylamide.

Table 2. Parameters of adsorption of polyacrylamide polymer chains onto the surface of TiO_2 nanoparticles

Sample	ΔH_{adh}^{∞}, J m^{-2}	K, g m^{-2}
TiO_2-P25	56.2	0.99
TiO_2- EEW	9.0	0.24

Figure 3a shows the dependence of the experimental enthalpy of dissolution of the composites, ΔH_3, on the weight fraction of TiO_2 nanoparticles in the composite.

As can be seen, ΔH_3 is negative for both samples of TiO_2 nanoparticles. The value at 0% filling corresponds to the enthalpy of dissolution of polyacrylamide (ΔH_1), which has a large negative value, –90 J g^{-1}. The value at 100% filling corresponds to the enthalpy of wetting of TiO_2 nanoparticles (ΔH_2), –5 J g^{-1}. At the TiO_2 nanoparticle content lower than 30%, the concentration dependence of ΔH_3 passes through a minimum; i.e., the composites in this composition range dissolve with a larger heat release than the individual polyacrylamide does. With a further increase in the TiO_2 fraction in the composite, ΔH_3 monotonically decreases in the absolute value. From the experimental data obtained, we calculated the enthalpies of mixing for the composites, ΔH_m. The dependence of ΔH_m on the degree of filling with TiO_2 nanoparticles is shown in Fig. 3b.

As seen from Fig. 3b, for both samples of TiO_2 nanoparticles the quantity ΔH_m is positive at all the degrees of filling, and its concentration dependence is dome-shaped with a maximum. For composites based on TiO_2-P25 nanoparticles, ΔH_m is more positive. The fact that the enthalpy of mixing of PAA/TiO_2 components depends on the concentration of TiO_2 nanoparticles is due to the fact that the adhesion layers on the nanoparticle surface are formed differently at different polymer/TiO_2 ratios. The concentration dependences obtained allow estimation of the enthalpy of adhesion of PAA polymer chains to the TiO_2 nanoparticle surface in saturated adsorption layers. To this end, we used a model that we developed previously, according to which the formation of an adhesion layer of polymer units on the filler particle surface is described by the equation similar to the well-known Langmuir equation

$$H_{adh} = \Delta H^{\infty}_{adh} \frac{Kc_{pol}}{1 + Kc_{po\text{-}l}},$$

where ΔH_{adh}^{∞} is the enthalpy of adhesion in the saturated adsorption layer on the particle surface; K, effective adsorption constant; and c_{pol}, polymer amount per 1 m^2 of the filler surface.

Apparently,

$$c_{pol} = \frac{1 - \omega_{fil}}{\omega_{fil} S_{sp}},$$

where ω_{fil} is the weight fraction of the filler in the composite, and S_{sp} is the specific surface area of the filler.

Thus, the contribution of adhesion interactions on the polymer/filler interface per gram of the composite can be calculated as follows:

$$\Delta H_m = \Delta H_{adh}\, \omega_{fil} S_{sp} = \Delta H_{adh}^{\infty} \frac{\omega_{fil}(1 - \omega_{fil})\, S_{sp}}{1 - \omega_{fil} + KS_{sp}\omega_{fil}} = \Delta H_{adh}^{\infty} \frac{\omega_{fil}\omega_{pol} S_{sp}}{\omega_{pol} + \omega_{fil} KS_{sp}},$$

where ω_{pol} is the weight fraction of the polymer in the composite.

According to this equation, the parameters characterizing the adhesion of PAA units to the filler (TiO_2 nanoparticle) surface (ΔH_{adh}^{∞} and K) can be calculated by nonlinear fitting of the experimental dependences of ΔH_m on the filling degree of filling of the composite. The lines in Fig. 3b reflect this fitting, and the corresponding parameters are given in Table 2.

As seen from Table 2, the limiting enthalpy of adhesion in the saturated adsorption layer, ΔH_{adh}^{∞}, is positive in both cases. This fact indicates that the interaction of PAA polymer chains with the TiO_2 nanoparticle surface is energetically unfavorable. Binary composites PAA/TiO_2 can be prepared, but in the presence of water, which is a third component of composite hydrogels, PAA polymer chains will not undergo spontaneous adsorption on the surface of TiO_2 nanoparticles.

Figure 4 shows the photomicrographs of composite hydrogels prepared as cylindrical samples.

As can be seen, TiO_2-P25 nanoparticles in the bulk of the hydrogel are aggregated to a greater extent than TiO_2-EEW nanoparticles, which are mostly uniformly distributed in the bulk of the hydrogel and cannot be

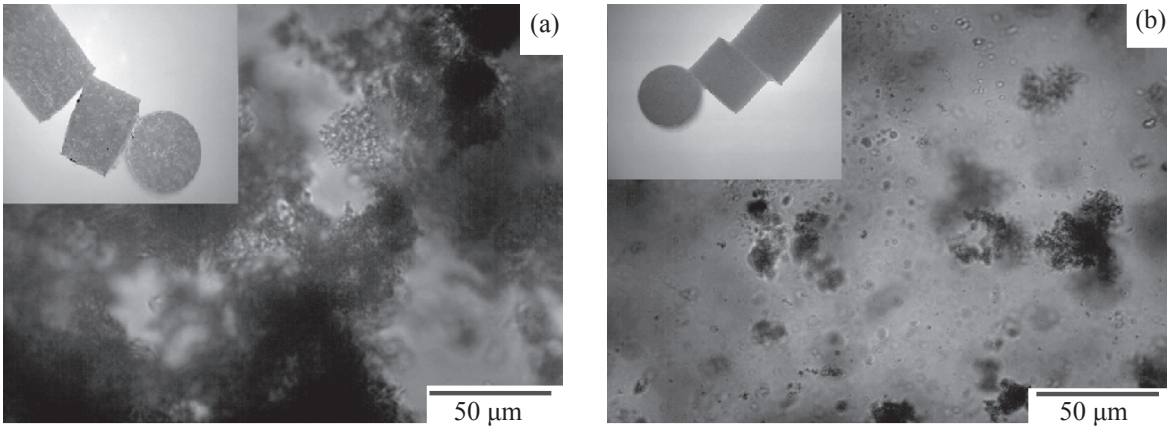

Fig. 4. Photomicrographs of composite hydrogels filled with (a) TiO_2-P25 and (b) TiO_2-EEW nanoparticles (magnification 400). The inserts show the hydrogel samples without magnification.

seen in the image, because the particle size is smaller than the resolving power of the optical microscope. Thus, thermodynamic incompatibility of TiO_2 with the PAA polymer network leads to the contraction of the interface area via aggregation. Because the PAA network interacts with the surface of TiO_2-P25 nanoparticles less efficiently than with the surface of TiO_2-EEW nanoparticles (Table 2), the aggregation of TiO_2-P25 nanoparticles in the bulk of the PAA hydrogel is more pronounced.

Thus, the polymer network of the PAA hydrogel does not interact with the surface of nanoparticles of both TiO_2 nanopowders. Presumably, the nanoparticles are "held" by the hydrogel polymer network without formation of any adhesion bonds, which makes probable the penetration of solute molecules to the photocatalytically active surface of the photocatalyst nanoparticles immobilized in the bulk of the hydrogel, with their subsequent photocatalytic decomposition under UV irradiation. Thus, the absence of the adhesion interaction of the hydrogel polymer network with photocatalyst nanoparticles is probably the necessary condition for their photocatalytic activity in the case of immobilization in a hydrogel. Otherwise, the adsorbed organic polymer units themselves would undergo photocatalytic decomposition more probably.

We examined the photocatalytic activity (PA) both of TiO_2 nanoparticles immobilized in the PAA hydrogel and of individual TiO_2 nanoparticles without hydrogel polymer matrix. Figure 5 shows how the MO concentration decreases with the time of UV irradiation in the presence of TiO_2 nanoparticles. The results are given for PA of TiO_2 nanoparticles immobilized in the hydrogel in comparison with PA of individual TiO_2 nanoparticles taken as a suspension. The amounts of TiO_2 nanoparticles were equivalent in both cases.

The dependences obtained were processed using a pseudo-first-order rate equation, and the effective rate constants k of decolorization of aqueous MO solution in the presence of TiO_2 nanoparticles under UV irradiation were calculated. The values obtained are given in Table 3.

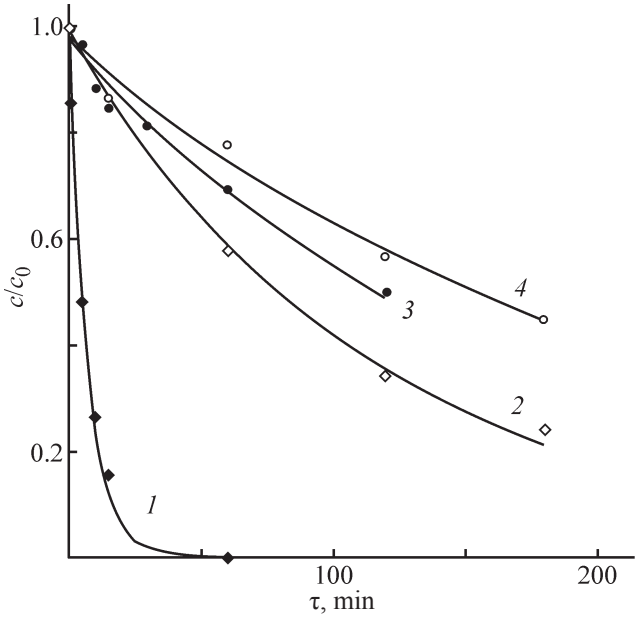

Fig. 5. The change in the concentration of Methyl Orange dye relative to the initial concentration, c/c_0, with the time τ of UV irradiation in the presence of individual (*1*) TiO_2-P25 and (*3*) TiO_2-EEW nanoparticles and of hydrogel-immobilized (*2*) TiO_2-P25 and (*4*) TiO_2-EEW nanoparticles.

Table 3. Effective rate constants of photocatalytic decomposition of Methyl Orange molecules under UV irradiation in aqueous medium on the surface of individual suspended TiO_2 nanoparticles and of TiO_2 nanoparticles immobilized in PAA hydrogel

Sample	Effective rate constant k, min^{-1}	
	individual suspended nanoparticles	nanoparticles immobilized in PAA hydrogel
TiO_2-P25	1.29×10^{-1}	8.1×10^{-3}
TiO_2- EEW	6.0×10^{-3}	4.3×10^{-3}

Figure 5 shows that, in both cases, the MO concentration decreases in the presence of TiO_2 nanoparticles under UV irradiation. This fact indicates that TiO_2 nanoparticles exhibit PA not only as individual nanoparticles in a suspension, but also as nanoparticles immobilized in the polymer network of the PAA hydrogel. On the whole, composite hydrogels based on TiO_2-P25 nanoparticles exhibit higher PA compared to the systems containing TiO_2-EEW nanoparticles. This fact is consistent with the results obtained previously for these TiO_2 nanoparticles. Comparison of the PA of the individual TiO_2 nanoparticles in a suspension and of TiO_2 nanoparticles immobilized in a hydrogel shows that the hydrogel polymer network influences the PA of TiO_2 nanoparticles differently. For example, in the case of TiO_2-P25 nanoparticles their PA decreases upon immobilization in the hydrogel. On the contrary, the PA of TiO_2-EEW nanoparticles immobilized in the hydrogel virtually coincides with that of the individual nanoparticles in a suspension. In other words, in the case of TiO_2-P25 nanoparticles the polymer network of the PAA hydrogel decreases their PA, which agrees with the data of [12], whereas in the case of TiO_2-EEW nanoparticles the hydrogel matrix does not noticeably affect their PA.

This difference can be accounted for as follows. Probably, photocatalytic decomposition of MO molecules under UV irradiation on the surface of TiO_2 nanoparticles immobilized in the hydrogel occurs in the diffusion mode. Apparently, the diffusion of MO molecules to the nanoparticle surface through the bulk of the hydrogel is hindered compared to the diffusion of MO molecules to the surface of individual nanoparticles suspended in an aqueous solution. Presumably, in the case of TiO_2-P25 nanoparticles the rate of photocatalytic decomposition of MO on the nanoparticle surface exceeds the rate of diffusion of MO molecules in the gel to the nanoparticle surface; i.e., the diffusion is the limiting step of the process. In the case of less photocatalytically active TiO_2-EEW nanoparticles, the rate of photocatalytic decomposition of MO on the nanoparticle surface is comparable to, or even lower than the rate of MO diffusion to the nanoparticle surface through the bulk of the hydrogel. Therefore, apparently, the polymer network of the PAA hydrogel does not affect the PA of the TiO_2-EEW nanoparticles. The prevalence of the diffusion control for TiO_2-P25 and kinetic control for TiO_2-EEW is probably due not only to different photocatalytic activity of the individual nanoparticles, but also to different character of nanoparticle aggregation in the hydrogel matrix.

CONCLUSIONS

Polyacrylamide-based chemically cross-linked composite hydrogels filled with photocatalytically active nanoparticles of commercial titanium dioxide (TiO_2-P25) and of titanium dioxide prepared by electrical explosion of a wire (TiO_2-EEW) were synthesized. As shown by thermochemical analysis, interaction of polyacrylamide chains with the surface of TiO_2 nanoparticles is energetically unfavorable. The photocatalytic activity of composite hydrogels evaluated by the decomposition of Methyl Orange model dye under UV irradiation in aqueous medium was studied. Because the polymer network of polyacrylamide does not interact with the surface of TiO_2 nanoparticles in the composite hydrogel, the surface remains open for the adsorption of dye molecules, which makes probable the photocatalytic decomposition of the dye molecules on the surface of TiO_2 nanoparticles immobilized in the bulk of the hydrogel. However, the polymer network of the polyacrylamide hydrogel hinders the diffusion of Methyl Orange molecules to the nanoparticle surface, which affects the photocatalytic activity of composite hydrogels in comparison with that of individual TiO_2 nanoparticles free of the hydrogel polymer matrix. In the case of TiO_2-P25 nanoparticles, the hydrogel polymer matrix decreases

their photocatalytic activity; i.e., the process is diffusion-controlled. In the case of less photocatalytically active TiO_2-EEW nanoparticles, the hydrogel polymer network does not affect their photocatalytic activity; i.e., the process is kinetically controlled. The homogeneity of the nanoparticle distribution and their aggregation in the bulk of the composite hydrogel are significant factors influencing the photocatalytic activity of TiO_2 nanoparticles immobilized in the polymer network of the polyacrylamide hydrogel.

The results obtained can be used for developing systems for photocatalytic water treatment, based on composite hydrogels filled with photocatalytically active TiO_2 nanoparticles.

ACKNOWLEDGMENTS

The authors are grateful to A.M. Murzakaev, A.I. Medvedev, O.M. Samatov, and A.G. Galyas for the assistance in performing the measurements. The study was financially supported in part by government assignment theme no. 0389-2014-0002.

REFERENCES

1. Schneider, J. et al., *Chem. Rev*., 2014, vol. 114, no. 19, pp. 9919–9986.
2. Li, C. et al., *Green Chem*., 2017, vol. 19, no. 4, pp. 882–899.
3. Truppi, A. et al., *Catalysts*, 2017, vol. 7, no. 4, pp. 100–133.
4. Low, J. et al., *Adv. Mater*., 2017, vol. 29, no. 20, pp. 1–20.
5. Srikanth, B. et al*., J. Environ. Manag.,* 2017, vol. 200, pp. 60–78.
6. Singh, S., Mahalingam, H., and Singh, P.K., *Appl. Catal. A: General*, 2013, vols. 462–463, pp. 178–195.
7. Colmenares, J.C. and Kuna, E., *Molecules,* 2017, vol. 22, no. 5, pp. 790–806.
8. Lei, P. et al., *J. Hazard. Mater.,* 2012, vols. 227–228, pp. 185–194.
9. Philippova, O.E., *Polym. Sci., Ser. C*, 2000, vol. 42, no. 2, pp. 208–228.
10. Kangwansupamonkon, W., Jitbunpot, W., and Kiatkamjornwong, S., *Polym. Degrad. Stab*., 2010, vol. 95, no. 9, pp. 1894–1902.
11. Tang, Q., et al., *Eur. Polym. J.,* 2007, vol. 43, no. 6, pp. 2214–2220.
12. Kazemi, F., Mohamadnia, Z., Kaboudin, B., and Karimi, Z., *J. Appl. Polym. Sci*., 2016, vol. 133, no. 19, pp. 43386–43395.
13. Wei, S. et al., *Polym. Polym. Compos*., 2016, vol. 16, no. 2, pp. 101–113.
14. Morsi, R.E. and Elsalamony, R.A., *New J. Chem.*, 2016, vol. 40, no. 3, pp. 2927–2934.
15. Zhang, D. et al., *Sci. Rep*., 2013, vol. 3, pp. 1399–1406.
16. Im, J.S., Bai, B.C., In, S.J., and Lee, Y.S., *J. Colloid Interface Sci.*, 2010, vol. 346, no. 1, pp. 216–221.
17. Yun, J., et al., *Mater. Sci. Eng. B: Solid-State Mater. Adv. Technol.,* 2011, vol. 176, no. 3, pp. 276–281.
18. Lučić, M. et al., *Sep. Purif. Technol*., 2014, vol. 122, pp. 206–216.
19. Shih, W.H., Hirata, Y., and Carty, W.M., *Colloidal Ceramic Processing of Nano-, Micro-, and Macro-Particulate Systems*, Westerville: Am. Ceram. Soc., 2012.
20. Zhang, Y. et al., *Water Res.,* 2008, vol. 42, nos. 8–9, pp. 2204–2212.
21. Treloar, L.R.G., *The Physics of Rubber Elasticity*, Oxford: Oxford Univ. Press, 2005.
22. Quesada-Pérez, M., Maroto-Centeno, J.A., Forcada, J., and Hidalgo-Alvarez, R., *Soft Matter,* 2011, vol. 7, no. 22, pp. 10536–10547.
23. Rubinstein, M. and Colby, R.H., *Polymer Physics,* Oxford: Oxford Univ. Press, 2003.